南京航空航天大学

论文集

（二〇一〇年）第44册

其他

（第1分册）

南京航空航天大学科技部编

二〇一一年五月

其 他

目录 1

序号	姓名	职称	单位	论文题目	刊物、会议名称	年、卷、期
1	韩艳铧	副教授	航天学院	A GPS Based Autonomous Attitude Determination and Nonlinear Adaptive Robustness Controller Design for Spacecraft	SPIE International Conference on Space Information Technology	2009 年开会，2010 年出版论文集
2	高有涛	讲师	航天学院	基于估计参数的飞行器编队飞行相对姿态控制	《控制理论与应用》	20102703
3	高有涛	讲师	航天学院	非合作目标编队飞行耦合动力学建模与六自由度控制研究	《南京航空航天大学学报》	20104202
4	高有涛	讲师	航天学院	基于角速度观测器的卫星编队飞行相对姿态控制技术研究	《宇航学报》	20103107
5	井庆丰	讲师	航天学院	Research and the Hardware Design of the UE-LMS Compensation Method for the Doppler Frequency Shift in the OFDM System	2010 3rd International Congress on Image and Signal Processing	20100006
6	井庆丰	讲师	航天学院	利用 Matlab/Simulink 仿真改进通信原理课教学的探索	黑龙江科技信息	20100012
7	李爽	副教授	航天学院	MCAV/IMU integrated navigation for the powered descent phase of Mars EDL	Advances in Space Research	20104605
8	李爽	副教授	航天学院	星际着陆自主障碍检测与规避技术	航空学报	20103108
9	李爽	副教授	航天学院	火星 EDL 导航、制导与控制技术综述与展望	宇航学报	20103103
10	李爽	副教授	航天学院	火星进入、下降与着陆技术的新进展——以“火星科学实验室”为例	航天返回与遥感	20103104
11	张小白 王惠南	博士 教授	航天学院	Characteristic comparison between two types of miRNA precursors in metazoan species	BioSystems	201010000
12	张小白 王惠南	博士 教授	航天学院	The Trypanosoma brucei MitoCarta and its regulation and splicing pattern during development	Nucleic Acids Research	20103821
13	刘海颖 王惠南	讲师 教授	航天学院	Research on Integrity Monitoring For Integrated GNSS/SINS System	Proceedings of the 2010 IEEE International Conference on Information and Automation	2010
14	陈志明	博士	航天学院	基于信息一致性的分布式卫星姿态	宇航学报	20103110

	王惠南	教授		同步研究		
15	陈志明 王惠南	博士 教授	航天学院	基于大气阻力的微小卫星编队控制	应用科学学报	20102802
16	钟　元 王惠南	博士 教授	航天学院	基于 fMRI 的逻辑运算脑功能效应连接	南京航空航天大学学报	20104204
17	钟　元 王惠南	博士 教授	航天学院	基于 Granger 因果检验和 PCA 的脑网络效应连接方法	华南理工大学学报（自然科学版）	20103801
18	杨现辉 王惠南	硕士 教授	航天学院	ICP 算法在 3D 点云配准中的应用研究	计算机仿真	20102708
19	汤同伟 王惠南	硕士 教授	航天学院	航天器交会对接位姿测量最优估计	四川兵工学报	20103102
20	钱　萍 王惠南	硕士 教授	航天学院	基于三目视觉测量的航天器交会对接相对位姿确定算法	宇航学报	20103106
21	杨志根 王惠南	硕士 教授	航天学院	基于 ICA 的颞叶癫痫背侧注意网络的研究	生物医学工程学杂志	20102404
22	王银 陆宇平	博士 正高	航天学院	月球返回舱跳跃再入弹道特性分析与优化设计	南京航空航天大学学报	2010 4201
23	宗鹏	教授	航天学院	An Improved Connection-Oriented Routing in LEO Satellite Networks	WASE International Conference on Information Engineering	2010 年第一卷
24	宗鹏	教授	航天学院	Analysis and Validation of a New Path Loss Model for LEO Satellite Communication Systems	International Conference on Computer Engineering and Technology	2010
25	宗鹏	教授	航天学院	Prediction and Compensation of Sun Transit in LEO Satellite System	2010 International Conference on Communication and Mobile Computing	2010
26	宗鹏	教授	航天学院	再入飞船通信环境建模研究	航天器环境工程	20102705
27	宗鹏	教授	航天学院	Distributed Interactive Simulation for Iridium Communication System Based on HLA and OPNET	2010 3rd International Conference on Computer and Electrical Engineering	2010
28	宗鹏	教授	航天学院	The analysis and simulation of communication network in Iridium system based on OPNET	IEEE International Conference on Information Management and Engineering	2010
29	宗鹏	教授	航天学院	基于 RWG 法分析考虑互耦的阵列方	现代雷达	20103206

				向特性		
30	宗鹏	教授	航天学院	Link analyzing and simulation of TDRSS based on OPNET	International Conference on Communication and Mobile Computing	2010
31	宗鹏	教授	航天学院	The Analysis and Compensation of The Mutual Coupling for The Adaptive Array Antenna	国际毫米波,微波会议 ICMMT2010	2010
32	南英	教授	航天学院	Global 4-D Trajectory Optimization for Sapcecraft	Science China	20105308)
33	黄国强 南英	博士 教授	航天学院	二级入轨空天飞机上升轨迹优化	宇航学报	20103103
34	黄国强 南英	博士 教授	航天学院	小推力深空探测轨道全局优化设计	航空学报	20103107
35	南英	教授	航天学院	美国 F-16C/D 战机火力控制系统与地形（威胁区）回避/地形跟踪系统特征简介	2010 年首届中国国防科技信息高峰论坛《学术论文集》	2010
36	刘燕斌	副教授	航天学院	空天飞行器乘波设计的概念研究	航空动力学报	20102511
37	刘燕斌	副教授	航天学院	弹道导弹突防策略进展	导弹与航天运载技术	2010 年 306 期
38	陈国云 魏志勇	博士 教授	航天学院	正比计数器漏电流研究	南京航空航天大学学报	20104205
39	陈国云 魏志勇	博士 教授	航天学院	核能推进航天器新方法	航天器环境工程	20102701
40	雷升杰 魏志勇	硕士 教授	航天学院	空间粒子探测器中一种微电流测量电路设计	宇航计测技术	20103006
41	盛庆红	讲师	航天学院	Research on Filtering of DEM Data Based on the Fisher Functions	ICCET. IEEE. 2010	2010
42	盛庆红	讲师	航天学院	基于Beta样条曲线的等高线绘制研究	测绘工程	20101906
43	盛庆红	讲师	航天学院	采用遥感影像的林地建模研究	计算机工程与应用	20104637
44	姬亭, 盛庆红	研究生, 讲师	航天学院	大重叠度影像的相关系数匹配精度分析	计算机应用	20103002
45	陈金宝	讲师	航天学院	月球探测器着陆性能若干影响因素分析	宇航学报	20103103
46	雷仲魁	副高	无人机院	马步哈密顿圈（骑士巡游）在图像置乱加密方法上的应用	小型微型计算机系统	20100005
47	雷仲魁	副高	无人机院	基于逆速高比补偿测高法的侦察目标定位	遥控遥测	20103106
48	黄爱凤	中级	无人机院	估算 YB-3 有机玻璃蠕变疲劳寿命的时间寿命分数法	南京航空航天大学学报	20104203
49	罗秋凤	副高	无人机院	飞行控制计算机采集处理系统的设计与实现	测控技术	20102908

50	尹海莲	中级	无人机院	Integration of Manufacturing Cost into Structural Optimization of Composite Wings	Chinese Journal of Aeronautics	20102306
51	尹海莲	中级	无人机院	含复合材料的飞机机体成本估算方法探讨	大型客机设计、制造与使用经济性研究学术会议	
52	李悦	副高	无人机院	无人机气液压发射原理试验研究	南京航空航天大学学报	20104206
53	姚铭	初级	无人机院	基于 CAD/CAE 技术的复合材料结构设计及优化技术在飞机设计中的应用	2010 复合材料结构设计与优化技术研讨会论文集	2010 年
54	李杰锋	中级	无人机院	可热处理强化泡沫铝合金的初步研究	热加工工艺	20103916
55	李杰锋	中级	无人机院	Design and Test of Two-way SMA Linear Actuator Based on One-way Shape Memory Effect	The 3rd NUAA-KAIST Joint Symposium on Aerospace Engineering	2010
56	王洪宪	初级	无人机院	飞机起落架收放疲劳实验系统设计及应用	实验力学	20102502
57	钱默抒	中级	无人机院	Robust Fault-tolerant Control for A Class Of Spacecraft rendezvous: Actuator Fault Case	ICIC：Express Letters Part B：Applications	20100102
58	陈小毛	副高	无人机院	一种宽频带模态识别算法的快速实现	南京航空航天大学学报	20104201
59	李志宇	副高	无人机院	基于混合变参数的执行机构故障容错控制	南京航空航天大学学报	20104201
60	诸燕平 黄大庆	博士 正高	无人机院	基于 AOA 的无线传感器网络节点定位算法	传感器与微系统	20102902
61	黄大庆	正高	无人机院	一种无线传感器网络自身节点定位算法	华中科技大学学报	20103810
62	黄大庆	正高	无人机院	基于小波变换和自适应加权的无人机侦察图像融合	遥控遥测	20103105
63	耿通奋	中级	无人机院	基于 simulink 的无人机自主飞行全程仿真研究	航空计算技术	20104005
64	牛　妍 肖前贵	硕士 正高	无人机院	无人机 SINS-GPS 定位信息融合系统设计	东南大学学报	2010 年第 40 卷增刊
65	李　浩 肖前贵	硕士 正高	无人机院	火箭助推无人机起飞发射段建模与仿真	东南大学学报	20104000
66	肖前贵	正高	无人机院	Adaptive Reconfiguration control for fighters based on weighted multiple-model-structure	Transactions of Nanjing University of Aeronautics and Astronautics	20100703
67	肖莉萍	中级	无人机院	高校军品型号研制质量管理	魅力中国	201004113

2. GPS BASED SPACECRAFT ATTITUDE AUTONOMOUS DETERMINATION

2.1 Basic Principle

This paper first discusses two groups of baselines aligned in two-dimensional plane, among which $\vec{b}_{1,2}$ is the longer one and $\vec{b}_{1,3}$, which is shorter than half of the carrier wave, is the other one. It is shown in Fig. 1. θ is the angle between $\vec{b}_{1,3}$ (or $\vec{b}_{1,2}$) and the reference line *AC*. Each antenna has same satellite clock error considering these antennas share a same GPS receiver. In addition, propagated error of every antenna is approximately equal due to the distance between every two antennas which can be neglected relative to that between antenna and GPS satellite, and then the single-difference carrier phase (SDCP) measurement equation can be given by the following expression

$$\delta\varphi^j{}_{1,2} = \frac{1}{\lambda}(\vec{E}^j \bullet \vec{b}_{1,2}) - N^j{}_{1,2} \tag{1}$$

The subscript "*1,2*" denotes the baseline $\vec{b}_{1,2}$ formed by antennas "*1,2*", "*j*" denotes the *j*th satellite, $\delta\varphi^j{}_{1,2} \triangleq \delta\varphi^j{}_1 - \delta\varphi^j{}_2$ is SDCP associated with the baseline $\vec{b}_{1,2}$ and the *j*th satellite, $N^j{}_{1,2} \triangleq N^j_1 - N^j_2$ is the single-differenced integer ambiguity associated with the baseline $\vec{b}_{1,2}$ and the *j*th satellite, λ is the wavelength of the GPS L2 carrier signal, and $\vec{E}^j$ is unit vector of the antennas to GPS satellite *j*. comparing with the distance between a GPS satellite and a antenna, the length of baseline can be neglected, so unit vector formed every antenna to the GPS satellite *j* is all denoted by $\vec{E}^j$.

In the process of attitude determination, $\delta\varphi^j{}_{1,2}$ can be measured, λ is known, and $\vec{E}^j$ can be determined uniquely according to GPS satellite ephemeris and the position of spacecraft. Obviously the determination of $N^j{}_{1,2}$ is the key to obtain $\vec{b}_{1,2}$.

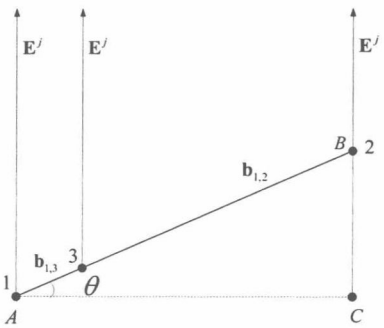

Fig. 1 Schematic of the Baseline vectors $\vec{b}_{1,2}$ and $\vec{b}_{1,3}$

2.2 The Determination of Integer Ambiguity and Baseline Vector $\vec{b}_{1,2}$

Then, we will determine the integer ambiguity of baseline $\vec{b}_{1,2}$ by means of the shorter baseline $\vec{b}_{1,3}$.

The SDCP measurement equation of $\vec{b}_{1,3}$ can be introduced as follows

$$\delta\varphi^j{}_{1,3} = \frac{1}{\lambda}(\vec{E}^j \bullet \vec{b}_{1,3}) - N^j{}_{1,3} \tag{2}$$

Owing to the length of $\vec{b}_{1,3}$ shorter than half of the carrier wave, so

$$\left|\vec{E}^j \bullet \vec{b}_{1,3}\right| < \frac{1}{2}\lambda \tag{3}$$

By substituting (3) in Eq. (2), we obtain

$$-\frac{1}{2} < N^{j}_{1,3} + \delta\varphi^{j}_{1,3} < \frac{1}{2} \tag{4}$$

By rounding in Eq. (4), we have

$$Int(N^{j}_{1,3} + \delta\varphi^{j}_{1,3}) = 0 \tag{5}$$

And then

$$N^{j}_{1,3} = 0 \tag{6}$$

That is, the integer ambiguity of baseline $\vec{b}_{1,3}$ whose length is shorter than half of the carrier wave is identically vanishing.

The following equation can be obtained by considering Eqs. (2) and (6) according to Fig. 1

$$\theta = \arcsin\frac{\delta\varphi^{j}_{1,3} \cdot \lambda}{|\vec{b}_{1,3}|} \tag{7}$$

Till then the azimuth angle of $\vec{b}_{1,3}$ can be determined uniquely.

But actually, the azimuth angle θ obtained by Eq.(7) has a deviation relative to its actual value because of various measurement errors included in $\delta\varphi^{j}_{1,3}$. Obviously, Eq. (7) shows that there is a positive correlation between precision of attitude determination and the length of baseline when carrier phase measurement errors are the same. Consequently, a new strategy is proposed by combining the advantages of shorter baseline which has no integer ambiguity and longer baseline which results in high precision. The detailed algorithm is as follows.

The following equation can be given by considering Eqs. (1) and (7) according to Fig. 1

$$\delta\varphi^{j}_{1,2} + N^{j}_{1,2} = \frac{|\vec{b}_{1,2}|\sin\theta}{\lambda} \tag{8}$$

Then the following equation can be obtained

$$N^{j}_{1,2} = \mathrm{int}(\frac{|\vec{b}_{1,2}|\sin\theta}{\lambda}) \tag{9}$$

The integer ambiguity of $\vec{b}_{1,2}$ is determined.

The precise value of azimuth angle of $\vec{b}_{1,2}$ can be given by considering Eqs. (1), (7) and (9) according to Fig. 1

$$\theta^{*} = \arcsin\frac{\lambda\left(\delta\varphi^{j}_{1,2} + \mathrm{int}\dfrac{|b_{1,2}|\,\delta\varphi^{j}_{1,3}}{|b_{1,3}|}\right)}{|b_{1,2}|} \tag{10}$$

In order to improve precision, four observed GPS satellites with minimum Geometric Dilution of Precision (GDOP) are selected to determine the precise attitude of $\vec{b}_{1,2}$, the observation equations are as follows

$$\begin{cases} \delta\varphi^1_{1,2} = \dfrac{1}{\lambda}(\bar{E}^1 \bullet \bar{b}_{1,2}) - N^1_{1,2} \\ \delta\varphi^2_{1,2} = \dfrac{1}{\lambda}(\bar{E}^2 \bullet \bar{b}_{1,2}) - N^2_{1,2} \\ \delta\varphi^3_{1,2} = \dfrac{1}{\lambda}(\bar{E}^3 \bullet \bar{b}_{1,2}) - N^3_{1,2} \\ \delta\varphi^4_{1,2} = \dfrac{1}{\lambda}(\bar{E}^4 \bullet \bar{b}_{1,2}) - N^4_{1,2} \end{cases} \tag{11}$$

Then the baseline vector $\vec{b}_{1,2}$ can be obtained from Eqs. (11) by least-squares pseudo inversion algorithm

$$\vec{b}_{1,2} = \lambda(E^T E)^{-1} E^T B_{1,2} \tag{12}$$

Where

$$E \triangleq \begin{bmatrix} E^1 \\ E^2 \\ E^3 \\ E^4 \end{bmatrix} \tag{13}$$

$$B_{1,2} \triangleq \begin{bmatrix} \delta\varphi^1_{1,2} + N^1_{1,2} \\ \delta\varphi^2_{1,2} + N^2_{1,2} \\ \delta\varphi^3_{1,2} + N^3_{1,2} \\ \delta\varphi^4_{1,2} + N^4_{1,2} \end{bmatrix} \tag{14}$$

Obviously, only yaw angle θ_2 and pitch angle θ_3 of spacecraft can be determined by $\vec{b}_{1,2}$, in order to determine roll angle θ_1, baselines $\vec{b}_{1,4}$ and $\vec{b}_{1,5}$ are arranged as Fig. 2.

In Fig.2, the length of $\vec{b}_{1,5}$ is shorter than half of the carrier wave, $\vec{b}_{1,4}$ is longer baseline. And then the azimuth angle of $\vec{b}_{1,4}$ can be obtained by the above method.

In the process of spacecraft's attitude Euler angles solution, GPS receiver antennas can be arranged as follows: antenna 1 is located at spacecraft mass center, antenna 2 and 3 are located along longitudinal toward spacecraft's head. Antenna 4 and 5 are located along lateral axis perpendicular to $\vec{b}_{1,2}$.

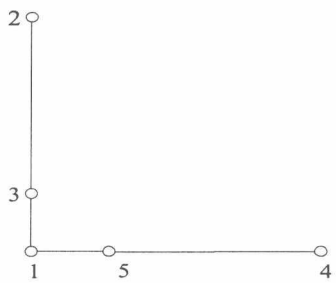

Fig. 2 Deployment diagram of the antennas

3. SPACECRAFT ATTITUDE CONTROL

3.1 The Attitude Motion Equation of Spacecraft

The attitude kinemics and dynamics equations are respectively as follows

$$\begin{cases} \dot{\theta}_1 = \omega_1 - \omega_2 \cos\theta_1 \tan\theta_3 + \omega_3 \sin\theta_1 \tan\theta_3 \\ \dot{\theta}_2 = \omega_2 \dfrac{\cos\theta_1}{\cos\theta_3} - \omega_3 \dfrac{\sin\theta_1}{\cos\theta_3} \\ \dot{\theta}_3 = \omega_2 \sin\theta_1 + \omega_3 \cos\theta_1 \end{cases} \tag{15}$$

$$\begin{cases} \dot{\omega}_1 = \dfrac{J_2 - J_3}{J_1}\omega_2\omega_3 + \dfrac{1}{J_1}(L_1 + f_1) \\ \dot{\omega}_2 = \dfrac{J_3 - J_1}{J_2}\omega_3\omega_1 + \dfrac{1}{J_2}(L_2 + f_2) \\ \dot{\omega}_3 = \dfrac{J_1 - J_2}{J_3}\omega_1\omega_2 + \dfrac{1}{J_3}(L_3 + f_3) \end{cases} \tag{16}$$

Where θ_1, θ_2, θ_3 are respectively spacecraft's roll, yaw and angle. ω_1, ω_2, ω_3 are corresponding respectively angle velocity. J_1, J_2, J_3 are respectively spacecraft three-axis inertia moment. L_1, L_2, L_3 are control torque, and f_1, f_2, f_3 are outer disturbance torque.

3.2 Design of Outer Loop Controller

Defining roll angle, yaw angle and pitch angle command are respectively θ_{1c}, θ_{2c} and θ_{3c}, attitude angles tracking error can be given by

$$\begin{cases} e_1 \triangleq \theta_1 - \theta_{1c} \\ e_2 \triangleq \theta_2 - \theta_{2c} \\ e_3 \triangleq \theta_3 - \theta_{3c} \end{cases} \tag{17}$$

The tracking error dynamic characteristics are designed as follows

$$\begin{cases} \dot{e}_1 + \mu_1 e_1 = 0 \\ \dot{e}_2 + \mu_2 e_2 = 0 \\ \dot{e}_3 + \mu_3 e_3 = 0 \end{cases} \tag{18}$$

Where, μ_1, μ_2, μ_3 are all positive constants, the following equations can be obtained by considering Eqs. (15), (17) and (18)

$$\begin{cases} \omega_1 = -\mu_1(\theta_1 - \theta_{1c}) - \mu_2(\theta_2 - \theta_{2c})\sin\theta_3 \\ \omega_2 = -\mu_2(\theta_2 - \theta_{2c})\cos\theta_1\cos\theta_3 - \mu_3(\theta_3 - \theta_{3c})\sin\theta_1 \\ \omega_3 = \mu_2(\theta_2 - \theta_{2c})\sin\theta_1\cos\theta_3 - \mu_3(\theta_3 - \theta_{3c})\cos\theta_1 \end{cases} \tag{19}$$

Let $\omega_1, \omega_2, \omega_3$ from Eqs. (19) be the attitude angle velocity commands, that is

$$\begin{cases} \omega_{1c} = \omega_1 \\ \omega_{2c} = \omega_2 \\ \omega_{3c} = \omega_3 \end{cases} \tag{20}$$

3.2 Design of Inner Loop Structure Adaptive Controller

Switching functions and reaching law are designed as follows

$$\begin{cases} s_1 \triangleq \omega_1 - \omega_{1c} \\ s_2 \triangleq \omega_2 - \omega_{2c} \\ s_3 \triangleq \omega_3 - \omega_{3c} \end{cases} \tag{21}$$

$$\begin{cases} \dot{s}_1 = -k_1 s_1 - \xi_1 \operatorname{sgn} s_1 \\ \dot{s}_2 = -k_2 s_2 - \xi_2 \operatorname{sgn} s_2 \\ \dot{s}_3 = -k_3 s_3 - \xi_3 \operatorname{sgn} s_3 \end{cases} \tag{22}$$

$$\begin{cases} L_1 = J_1 z_1 - (J_2 - J_3)\omega_2\omega_3 - f_1 \\ L_2 = J_2 z_2 - (J_3 - J_1)\omega_3\omega_1 - f_2 \\ L_3 = J_3 z_3 - (J_1 - J_2)\omega_1\omega_2 - f_3 \end{cases} \tag{23}$$

$$\begin{cases} z_1 \triangleq \omega_{1c} - k_1 s_1 - \xi_1 \operatorname{sgn} s_1 \\ z_2 \triangleq \omega_{2c} - k_2 s_2 - \xi_2 \operatorname{sgn} s_2 \\ z_3 \triangleq \omega_{3c} - k_3 s_3 - \xi_3 \operatorname{sgn} s_3 \end{cases} \tag{24}$$

$$\begin{cases} L_1 = \hat{J}_1 z_1 - (\hat{J}_2 - \hat{J}_3)\omega_2\omega_3 - \hat{f}_1 \\ L_2 = \hat{J}_2 z_2 - (\hat{J}_3 - \hat{J}_1)\omega_3\omega_1 - \hat{f}_2 \\ L_3 = \hat{J}_3 z_3 - (\hat{J}_1 - \hat{J}_2)\omega_1\omega_2 - \hat{f}_3 \end{cases} \tag{25}$$

Where k_1, k_2, k_3, ξ_1, ξ_2, ξ_3 are all positive constants.

The control torque can be given by the following expressions by considering Eqs. (16), (21) and (22)

Where

J_1, J_2, J_3 and f_1, f_2, f_3 in Eqs. (23) are all uncertain, thus control law introduced in Eqs. (23) is difficult to realize, therefore, we substitute the estimate $\hat{J}_1$, $\hat{J}_2$, $\hat{J}_3$, $\hat{f}_1$, $\hat{f}_2$, $\hat{f}_3$ for J_1, J_2, J_3, f_1, f_2, f_3, and then the control law can be written as follows

The following equations can be derived from Eqs. (16), (21), (24) and (25)

$$\begin{cases} \dot{s}_1 + k_1 s_1 + \xi_1 \operatorname{sgn} s_1 = \dfrac{1}{J_1}(\tilde{J}_1 z_1 - \tilde{J}_2\omega_2\omega_3 + \tilde{J}_3\omega_2\omega_3 - \tilde{f}_1) \\ \dot{s}_2 + k_2 s_2 + \xi_2 \operatorname{sgn} s_2 = \dfrac{1}{J_2}(\tilde{J}_1\omega_3\omega_1 + \tilde{J}_2 z_2 - \tilde{J}_3\omega_3\omega_1 - \tilde{f}_2) \\ \dot{s}_3 + k_3 s_3 + \xi_3 \operatorname{sgn} s_3 = \dfrac{1}{J_3}(-\tilde{J}_1\omega_1\omega_2 + \tilde{J}_2\omega_1\omega_2 + \tilde{J}_3 z_3 - \tilde{f}_3) \end{cases} \tag{26}$$

Where

$$\begin{cases} \tilde{J}_1 \triangleq \hat{J}_1 - J_1 \\ \tilde{J}_2 \triangleq \hat{J}_2 - J_2 \\ \tilde{J}_3 \triangleq \hat{J}_3 - J_3 \\ \tilde{f}_1 \triangleq \hat{f}_1 - f_1 \\ \tilde{f}_2 \triangleq \hat{f}_2 - f_2 \\ \tilde{f}_3 \triangleq \hat{f}_3 - f_3 \end{cases} \tag{27}$$

denotes estimate error.

Defining

$$S \triangleq (s_1, s_2, s_3)^T \tag{28}$$

$$K \triangleq \begin{bmatrix} k_1 & 0 & 0 \\ 0 & k_2 & 0 \\ 0 & 0 & k_3 \end{bmatrix} \tag{29}$$

$$J \triangleq \begin{bmatrix} J_1 & 0 & 0 \\ 0 & J_2 & 0 \\ 0 & 0 & J_3 \end{bmatrix} \tag{30}$$

$$\xi \triangleq \begin{bmatrix} \xi_1 & 0 & 0 \\ 0 & \xi_2 & 0 \\ 0 & 0 & \xi_2 \end{bmatrix} \tag{31}$$

$$W \triangleq \begin{bmatrix} z_1 & -\omega_2\omega_3 & \omega_2\omega_3 & -1 & 0 & 0 \\ \omega_3\omega_1 & z_2 & -\omega_3\omega_1 & 0 & -1 & 0 \\ -\omega_1\omega_2 & \omega_1\omega_2 & z_3 & 0 & 0 & -1 \end{bmatrix} \tag{32}$$

$$\tilde{P} \triangleq (\tilde{J}_1, \tilde{J}_2, \tilde{J}_3, \tilde{f}_1, \tilde{f}_2, \tilde{f}_3)^T \tag{33}$$

Then, Eqs. (26) can be written as matrix type

$$\dot{S} + KS + \xi \operatorname{sgn} S = J^{-1} W \tilde{P} \tag{34}$$

Consider the Lyapunov function as follows

$$V = \frac{1}{2} S^T J S + \frac{1}{2} \tilde{P}^T \gamma^{-1} \tilde{P} \tag{35}$$

Where γ is an arbitrary (6×6) symmetric positive definite matrix, for simplicity, we design γ to be a diagonal matrix

$$\gamma = \begin{bmatrix} \gamma_1 & 0 & 0 & 0 & 0 & 0 \\ 0 & \gamma_2 & 0 & 0 & 0 & 0 \\ 0 & 0 & \gamma_3 & 0 & 0 & 0 \\ 0 & 0 & 0 & \gamma_4 & 0 & 0 \\ 0 & 0 & 0 & 0 & \gamma_5 & 0 \\ 0 & 0 & 0 & 0 & 0 & \gamma_6 \end{bmatrix} \tag{36}$$

Derivative of Lyapunov function and consider Eq. (34), the following equation can be obtained

$$\dot{V} = -S^T JKS - S^T J \xi \operatorname{sgn} S + S^T W \tilde{P} + \tilde{P}^T \gamma^{-1} \dot{\tilde{P}} \tag{37}$$

If we choose adaptive law as follows

$$S^T W \tilde{P} + \tilde{P}^T \gamma^{-1} \dot{\tilde{P}} = 0 \tag{38}$$

By substituting Eq. (38) in Eq. (37), we obtain $\dot{V} = -S^T JKS - S^T J \xi \operatorname{sgn} S < 0$

And then the adaptive control law for parameter estimate can be derived from Eq. (38)

$$\dot{\tilde{P}} = -\gamma W^T S \tag{39}$$

4. NUMERICAL SIMULATION

Numerical simulation research about the integrated attitude close loop composed of determination system and control system. The attitude angles commands are square wave unit with amplitude 60° and period 10s. White Gaussian noise substitutes measurement error. The sampling period is set to 0.01s, the simulation time is 50s. Other simulation parameters are listed in Table 1. the simulation results are shown in Fig. 3~Fig. 6.

Table 1 Simulation parameters

Three-axis inertia moment nominal($kg \cdot m^2$)	$J^*_1 = 1200$ $J^*_2 = 2200$ $J^*_3 = 3100$
Three-axis inertia perturbed value($kg \cdot m^2$)	$\Delta J_1 = -500$ $\Delta J_2 = -800$ $\Delta J_3 = -1000$
Outer disturbance torque ($kg \cdot m^2$)	$f_1 = f_2 = f_3 = 500$
Spacecraft orbital elements	Semi-major axis: $a = 9 \times 10^3 (km)$ Numerical eccentricity: $e = 0.2$ Orbital inclination: $i = 30^\circ$ Argument of perigee: $\omega = 30^\circ$ Longitude of ascending node: $\Omega = 40^\circ$ Mean anomaly: $M_0 = 0^\circ$
Geocentric gravitational constant	$\mu = 3.986 \times 10^5$ (km^3/s^2)
GPS carrier wave length (m)	$\lambda = 0.24$
Baseline length (m)	$\lvert\vec{b}_{1,2}\rvert = 8.8$ $\lvert\vec{b}_{1,3}\rvert = 0.1$ $\lvert\vec{b}_{1,4}\rvert = 10$ $\lvert\vec{b}_{1,5}\rvert = 0.12$ $\mu_1 = \mu_2 = \mu_3 = 4$ $k_1 = k_2 = k_3 = 16$ $\xi_1 = \xi_2 = \xi_3 = 3$ $\gamma_1 = \gamma_2 = \gamma_3 = 500$ $\gamma_4 = 4000$ $\gamma_5 = \gamma_6 = 8000$
Mean molar quantity radius of the earth (km)	$r = 6400$
GPS satellites orbital elements	Semi-major axis: $a_G = 2.65 \times 10^4 (km)$ Numerical eccentricity: $e_G = 0.02$ Orbital inclination: $i_G = 55^\circ$ Argument of perigee: $\omega_G = 30^\circ$

Mean anomaly of GPS satellites: (°)	0; 90; 180; 270 20; 110; 200; 290 40; 130; 220; 310 60; 150; 240; 330 80; 170; 260; 350 100; 190; 280; 370
Longitude of ascending node of each plane at 0 o'clock, July 1, 1993 (°)	32.8; 92.8; 152.8; 212.6; 272.8; 332.8
White Gaussian noise parameters	Mean: 0 Variance: $\sigma^2 = 1$
Initial conditions	$\theta_{10} = \theta_{20} = \theta_{30} = 0^\circ$ $\omega_{10} = \omega_{20} = \omega_{30} = 0(\text{rad/s})$ $\hat{J}_{10} = 1200(\text{kg}\cdot\text{m}^2)$ $\hat{J}_{20} = 2200(\text{kg}\cdot\text{m}^2)$ $\hat{J}_{30} = 3100(\text{kg}\cdot\text{m}^2)$ $\hat{f}_1 = \hat{f}_2 = \hat{f}_3 = 0(\text{kg}\cdot\text{m}^2)$

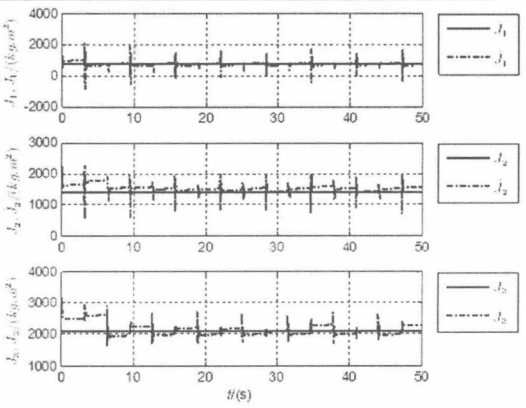

Fig. 3 The Actual Values and Estimates of Three-axis Inertia Moment

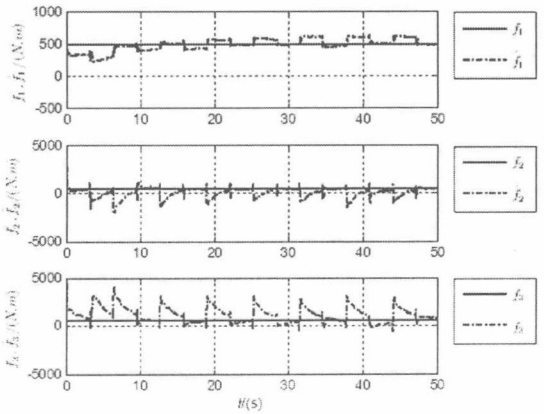

Fig. 4 The Actual Values and Estimates of Outer Disthurbance Torque

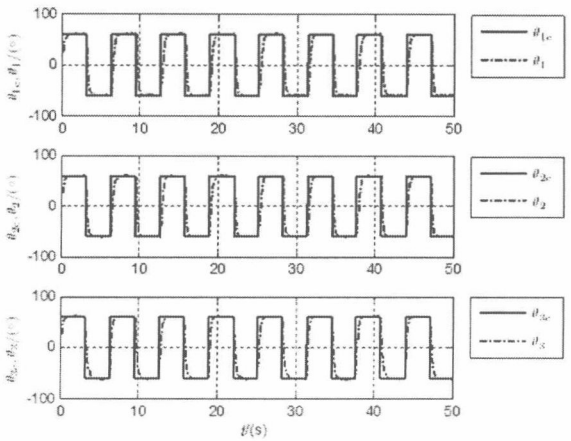

Fig. 5 Commands and Responses of Attitude Angles

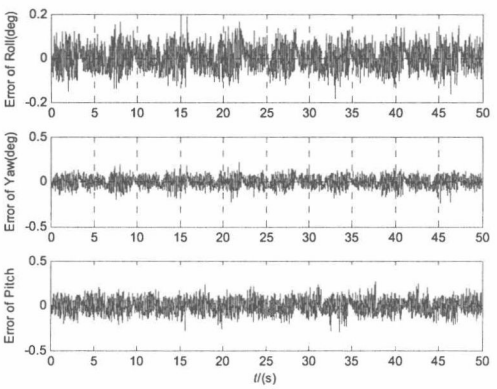

Fig. 6 Attitude Estimation Errors Based on GPS

5. CONCLUSIONS

Theoretical analyses and simulation results indicate that the integrated closed loop composed of determination system and control system has high precision and strong robustness. The estimate error for uncertain parameters is bounded, and the three-axis attitude Euler angles commands can be tracked quickly.

REFERENCES

1. Wang Huinan, "*Principles and Applications of GPS Navigation*," Beijing: Press of Science, 2003.
2. Xu Jiangning, Zhu Tao, "Review on GPS Attitude Determination," *Journal of Naval University of Engineering*, no. 3, pp. 17-22, 2003.
3. Lachapelle G, Lu G, Cannon M E, "Performance analysis of a shipborne gyrocompass with a multi-antenna system," Plans, New York: IEEE, pp. 337-343, 1994.
4. Juang J C, Huang G S, "Development of GPS-based attitude determination algorithms," *IEEE Transactions on Aerospace and Electronic Systems*, vol. 33, no. 3, pp. 968-976,1997.

5. Remodn B W, "Applying kinematic GPS techniques at our nation's airports," Plans, New York: IEEE, pp. 262-266, 1990.
6. M.Bahrami, and R.Kalantari Nezhad, "Adaptive Attitude Control of a Flexible Satellite," *Systems and Control in Aerospace and Astronautics*, pp. 1329-1333, 2006.
7. Zhou Fengqi, Han Yanhua, Zhou Jun. "Design of Robust Analysis for Spacecraft Attitude Controller," *Chinese Space Science and Technology*, no. 2, pp. 36-41, 2007.
8. Zhou Fengqi, Han Yanhua, Zhou Jun. "Design of Robust Analysis for Spacecraft Attitude Controller," *Chinese Space Science and Technology*, no. 2, pp. 36-41, 2007.
9. Georee B B, Fasse D E, "Sliding Mode Attitude Control of a Small Satellite for Ground Tracking Maneuvers," *Proceedings of the American Control Conference*, Chicago, pp. 1134-1138, June, 2000.
10. Hedrick J K, Gopalswamy S, 'Nonlinear flight control design via sliding methods," *Journal of Guidance*, pp. 492-505, 1991.

第 27 卷第3 期
2010 年 3 月

控 制 理 论 与 应 用
Control Theory & Applications

Vol. 27 No. 3
Mar. 2010

文章编号: 1000−8152(2010)03−0283−06

基于估计参数的飞行器编队飞行相对姿态控制

高有涛[1], 陆宇平[1,2], 徐 波[2]

(1. 南京航空航天大学 自动化学院, 江苏 南京 210016; 2. 南京航空航天大学 航天学院, 江苏 南京 210016)

摘要: 本文建立了空间飞行器编队飞行的相对姿态动力学模型, 用姿态四元数表示的动力学模型避免了大角度相对姿态变化时的奇异问题. 利用Lyapunov理论控制方法, 设计了带神经网络参数估计器的自校正控制器, 减轻了编队飞行器的测量和通信负担. 证明了控制器对模型误差具有较好的鲁棒性. 仿真结果验证了参数估计器可以准确的估计未知参数; 基于估计参数的控制器可以实现相对姿态的较精确控制.

关键词: 相对姿态; 神经网络; 参数估计; 自校正控制器

中图分类号: V412.4　　文献标识码: A

Parameter-estimation-based control for relative attitude of spacecraft formation flying

GAO You-tao[1], LU Yu-ping[1,2], XU Bo[2]

(1. College of Automation Engineering, Nanjing University of Aeronautics and Astronautics, Nanjing Jiangsu 210016, China;
2. College of Astronautics, Nanjing University of Aeronautics and Astronautics, Nanjing Jiangsu 210016, China)

Abstract: A relative attitude model represented by a quaternion is presented for the spacecraft formation flying. This model can avoid singularities. A self-tuning controller with a neural network estimator is proposed to reduce the measuring equipment and communications between spacecrafts in a formation flying. It is proved that the control system has good robustness to uncertainties of system model. Simulation results illustrate that the estimator can successfully estimate the unknown parameters and the relative attitude can be controlled accurately.

Key words: relative attitude; neural network; parameter estimation; self-tuning controller

1 引言(Introduction)

空间飞行器编队飞行的任务大多会依靠编队飞行器间的相互姿态配合完成, 例如, 卫星编队组成的SAR雷达, 要求每颗卫星的合成孔径雷达天线在指定的位置以指定的相对姿态指向空间某个方向; 又如美国早期由EO-1和LandSat7两颗卫星组成的编队, 要求编队卫星在一天或两天之内必须同时指向地球表面的某一点. 因此, 研究空间飞行器编队飞行的相对姿态运动具有重要的现实意义. Ahmed[1]研究了卫星编队飞行的姿态运动, 利用式$J\dot{\omega}+\omega\times(J\omega)=T$给出了卫星编队飞行的姿态运动模型, 姿态系统的理想状态为角速度的函数, 基本原理就是保持和跟踪一个理想的角速度. 基于这个模型, 文献[2]设计了一个利用模糊方法和H_2/H_∞方法结合的自适应控制器, 限制了外部干扰和模糊近似误差对姿态的影响, 减小了跟踪误差, 降低了燃料消耗; Kim[3]提出了一种与干扰相关的滑模控制方法, 比一般的滑模控制方法在减小稳态误差方面控制的更好; 文献[4]利用相对姿态运动学和动力学方程, 将跟踪控制问题转化为常规控制问题, 设计了相应的控制器. 文献[5,6]研究了主从星相对轨道参数和姿态角很小的情况下的卫星编队飞行相对姿态运动, 但用欧拉角表示的相对姿态运动可能会出现奇异情况. 文献[7]采用修改的Rodrigues参数表示相对姿态矩阵, 将姿态状态的跟踪控制设计问题转变成姿态状态控制的调节器设计问题. 以上研究均假设参与编队飞行的飞行器轨道是已知的, 飞行器的姿态角和角速度都是可以测量得到的. 但实际上, 模型中有些参数是无法测量的, 或者需要安装额外的测量设备或增加飞行器之间的通信量.

本文针对空间飞行器编队飞行相互姿态配合的情况, 建立了空间飞行器编队飞行相对姿态动力学模型. 用姿态4元数表示的动力学模型避免了大角度相对姿态变化时的奇异问题. 利用Lyapunov理论设计的非线性控制器将参考飞行器的参数作为未知

收稿日期: 2009−04−24; 收修改稿日期: 2009−06−26.
基金项目: 国家“863”计划资助项目(2008AA12Z301).